Electronic shell energies and deformations in large sodium clusters from evaporation spectra

F. Chandezon,* S. Bjørnholm, J. Borggreen, and K. Hansen†
The Niels Bohr Institute, Risø, DK-4000 Roskilde, Denmark
(Received 3 June 1996; revised manuscript received 28 October 1996)

Abundances of sodium clusters resulting from evaporation *in vacuo* of a large ensemble are analyzed quantitatively. Electronic shell structure gives rise to oscillations in the abundance distributions with maxima at the shell closings. From this, atomic separation energies and shell energies are derived from clusters with 50–230 atoms. The experimental shell energies are 2–3 times smaller in amplitude than calculated theoretically for spherical clusters. The discrepancy is understood as the result of deformations of the nonmagic clusters. In addition, the energy oscillations due to shell structure are extracted from (i) the atomic separation energies and (ii) the ionization potentials of clusters with sizes up to 110 electrons. The two quantities are compared and found to be nearly identical. [S0163-1829(97)08507-X]

INTRODUCTION

The electronic shell structure in metal clusters was discovered in 1984 as sawtoothlike oscillations in the abundance spectra of sodium clusters produced by an adiabatic expansion source.[1] Such shells are associated with spherical symmetry of the electronic mean field and hence with the shape of the cluster. Clusters with partly filled shells will be deformed (the Jahn-Teller effect), and a qualitative indication for this was found in the initially measured abundances for cluster sizes up to $N=40$.[2] Later, shell structure and deformations were observed for several other metallic elements.[3] The characteristic shell oscillations have been identified experimentally up to very large sizes, but to our knowledge a quantitative analysis of the abundance spectra in terms of shell energies has been lacking for clusters larger than about 40 atoms. Here we present an analysis of this kind.

I. FROM EVAPORATION SPECTRA TO ELECTRONIC SHELLS ENERGIES

The question of the quantitative relation between cluster abundances and shell variations in the atomic binding energies was already addressed by de Heer *et al.*,[4] later by Bjørnholm *et al.*,[5] and also in the more recent review by de Heer.[3] None of these treatments leads to definite conclusions, and they all made the erroneous assumption that all clusters in an ensemble could be thought to possess the same temperature at a given time irrespective of size. It has since then become clear that the abundance spectra in question are generated by a process of evaporation in vacuum, where the average cluster temperature oscillates with cluster size.[6] An ensemble of clusters that have undergone several evaporations in vacuum prior to mass analysis fulfills the requirements of an evaporative ensemble as discussed by Klots.[7] The clusters follow distinct decay chains depending on their initial mass and energy and the abundances measure the amount of these chains that have terminated at the respective sizes at the moment of observation; see Fig. 1.

How does the connection between the abundances and the electronic shell structure arise? The rate of evaporation of an atom is sensitive to the separation energy $D(N)$ (>0), i.e., the energy required to remove an atom from a cluster of size N. If $E(N)$ (<0) is the cohesive energy of the same cluster then

$$D(N)=E(N-1)-E(N). \tag{1}$$

Following Strutinsky,[8] the cohesive energy can be written as

$$E(N)=\tilde{E}(N)+E_{\text{shell}}(N), \tag{2}$$

where the first term is a smooth bulklike contribution and the second one, the *shell energy*, is an oscillating term due to electronic shell structure and deformations. The minima of

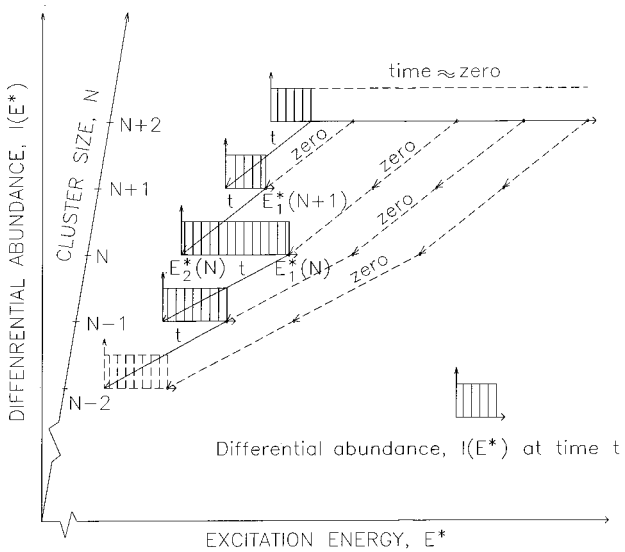

FIG. 1. Illustration of the Klots model for small clusters: only the last evaporation step in each decay chain needs to be considered (full lines marked t). The relative abundance is equated to the width of the interval of excitation energies existing in cluster N at time t. This interval is bracketed by two lines marked t, one feeding and the other depopulating a cluster of a given size. In the graph, the separation energy increases abruptly between sizes $N+1$ and N. This results in an extra contribution to the cluster N, as expressed in the second term of Eq. (9).

$E_{\text{shell}}(N)$ correspond to especially stable clusters with closed electronic shells. From Eqs. (1) and (2), it follows that also the separation energy is a sum of two terms $\tilde{D}(N)$ and $D_{\text{shell}}(N)$ with

$$D_{\text{shell}}(N)=E_{\text{shell}}(N-1)-E_{\text{shell}}(N). \tag{3}$$

Therefore, a closed shell corresponds to a change of sign of the function $D_{\text{shell}}(N)$. This is confirmed in several calculations:[9–11] at zero temperature, the $D_{\text{shell}}(N)$ function is composed of sawteeth with steep downward steps at the shell closings; at finite temperature, the steps are replaced by S-shaped curves with inflection points still at the shell closings.

The shell energy must then obviously be reflected in the mass spectra of clusters evaporating in vacuum, but it is only recently that a satisfactory quantitative analysis has become possible. By extending Klots's work to include large clusters, Hansen and Näher have developed a general model applicable to an evaporative ensemble *in vacuo* for the case of monomer evaporation being the only decay channel.[12]

For small clusters ($N\lesssim 100$), the specific Klots assumption is valid: the clusters of size N that one observes at time t are the end products of evaporative chains, where all steps except the last one—from $N+1$ to N—can be considered as instantaneous (see Fig. 1).[7] The abundance $I(N)$ at time t is then determined by the length of the interval of internal energies $E_1^*(N)-E_2^*(N)$ of clusters of size N present at time t. Here $E_1^*(N)$ is the energy of the hottest cluster surviving at time t. Its decay constant is $k_1(N)=1/t$. The quantity $E_2(N)$ is the energy of the last arrived cluster N. It originates from the cluster $N+1$ with energy $E_1^*(N+1)$ and decay constant $k_1(N+1)=1/t$. If we assume an Arrhenius-type decay rate

$$k(N)=\omega N^{2/3}\exp\left(-\frac{D(N)}{k_B T(N)}\right), \tag{4}$$

where ω is the Debye frequency of the material and $T(N)$ the canonical temperature of the cluster N corresponding to an average internal energy $E^*(N)$, this leads to

$$\frac{D(N)}{T_1(N)}=\frac{D(N+1)}{T_1(N+1)}=k_B\ln(\omega N^{2/3}t)\equiv k_B G$$

$$\Leftrightarrow T_1(N+1)-T_1(N)=\frac{D(N+1)-D(N)}{k_B G}, \tag{5}$$

where G, the so-called Gspann factor, is typically of order 20–30. With

$$E_2^*(N)=E_1^*(N+1)-D(N+1) \tag{6}$$

and assuming Dulong and Petit's value for the heat capacity C_v, i.e.,

$$E^*(N)=(3N-6)k_B T(N)\approx 3Nk_B T(N), \tag{7}$$

the relation between the abundance of the cluster size N and the separation energy is

$$I(N)\propto E_1^*(N)-E_2^*(N)=D(N+1)-[E_1^*(N+1)-E_1^*(N)]$$

$$=D(N+1)-\frac{3N}{G}[D(N+1)-D(N)]. \tag{8}$$

It is not necessary to assume step functions for the decay rates at energies $E_1^*(N)$ and $E_2^*(N)$ as here. Taking a more realistic smooth dependence of $k(N)$ with $E^*(N)$ also results in expression (8).

The formula (8) is more conveniently expressed in terms of relative (i.e., dimensionless) abundances and separation energies:

$$I_{\text{rel}}(N)=D_{\text{rel}}(N+1)-\frac{3N}{G}[D_{\text{rel}}(N+1)-D_{\text{rel}}(N)]. \tag{9}$$

Here the relative abundance $I_{\text{rel}}(N)=I(N)/\tilde{I}(N)$ corresponds to the measured abundance normalized to an appropriately smoothened distribution $\tilde{I}(N)$. The relative separation energy $D_{\text{rel}}(N)$ equals $D(N)/\tilde{D}(N)$. These functions oscillate around unity and contain the information about the shell structure.

For large clusters, several steps in each decay chain should be taken into account. The complete formula connecting $I(N)_{\text{rel}}$ to $D(N)_{\text{rel}}$ then contains a sum over all prior evaporation steps. If, however, the separation energy is a reasonably smooth function of size, the formula reduces to Eq. (9); see Ref. 12. In this case, t is a slightly N-dependent effective cooling time, but since it appears in the logarithm this has no practical importance.

Recent experimental studies in the size range $N\lesssim 400$ have made it clear that previously measured abundance spectra obtained with an adiabatic expansion source acquire their final shape, in particular their shell oscillations, by evaporation in vacuum during the flight from the source to the point of ionization.[6,13] For sizes beyond $N=50$, where irregular dimer decay can be neglected,[14] the spectra can therefore be analyzed according to the formalism of Ref. 12. We have done so and found that (i) the spectra [see, e.g., Fig. 2(a)] are smooth enough to ensure that Eq. (9) is a valid approximation for all sizes and (ii) irrespective of size, the second term in Eq. (9) is the dominant one near the shell closings. In view of the sawtooth, or S-shaped, form expected for the $D(N)$ function this means that a shell closure should appear as a maximum in the relative abundance spectrum.

In order to obtain quantitative results the relative intensities $I_{\text{rel}}(N)$ are first turned into relative separation energies $D_{\text{rel}}(N)$ by simply inverting Eq. (9) numerically. The $D_{\text{rel}}(N)$ values can be converted to absolute energy units by assuming that the average separation energy $\tilde{D}(N)$ is equal to the bulk cohesive energy of liquid sodium, which is very close to 1.0 eV. The measured relative abundances and the separation energies derived from these are shown in Fig. 2. One sees that the positions of the inflection points (steepest descent) in the function $D(N)$ coincide with maxima in the abundance curve as anticipated.

A comparison with the results of calculations is most conveniently made in terms of the (Strutinsky) shell energies, $E_{\text{shell}}(N)$. This quantity is obtained by integration:

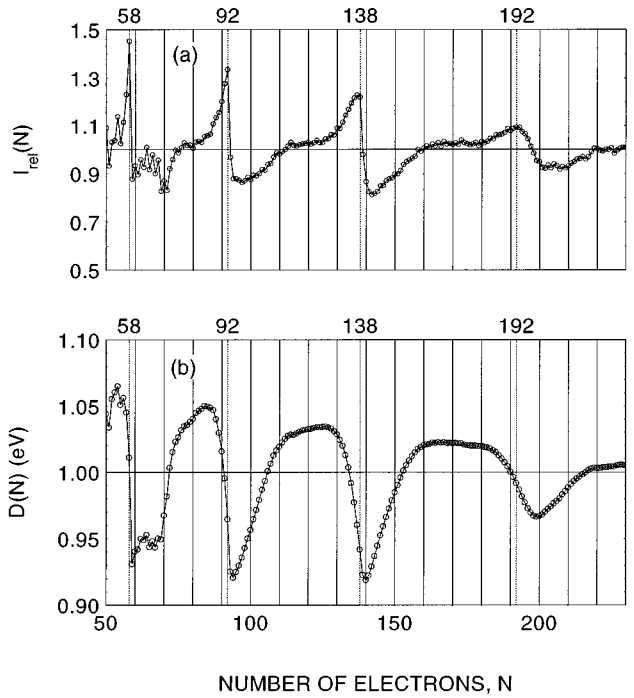

FIG. 2. (a) Relative abundances $I(N)_{\mathrm{rel}}$ of sodium clusters (Ref. 13), (b) separation energies $D(N)$ obtained from the data of (a) using Eq. (9) and normalizing to an average value of 1 eV. The evaporation time is $t \approx 1$ ms, and ω, the Debye frequency, is equal to 3.3×10^{12} Hz (Ref. 28). The magic numbers identified as the inflection points of the downsloping part of the $D(N)$ curve are indicated on the upper x axes.

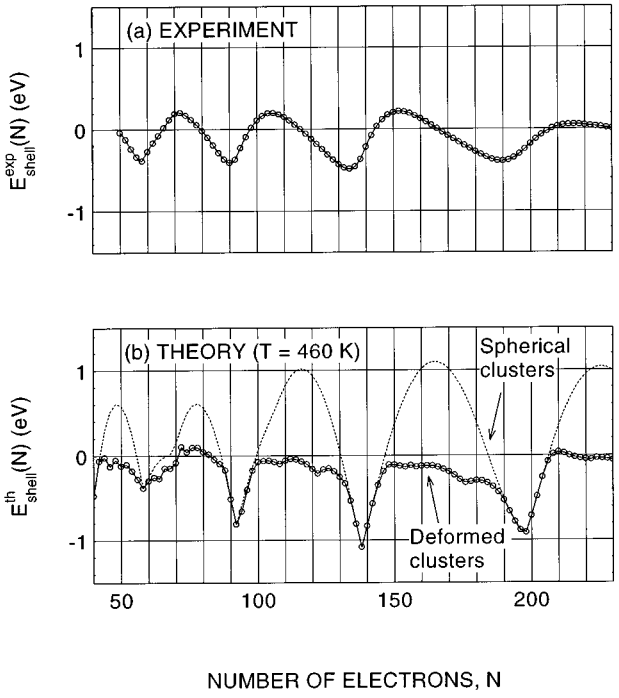

FIG. 3. (a) Experimental shell energies deduced from the data in Fig. 2(b) compared to (b) theoretical shell energies for spherical (dotted curve) and axially deformed clusters (○), respectively, from Ref. 11. Marks correspond to clusters with even sizes.

$$E_{\mathrm{shell}}(N) = -\sum_{i=2}^{N} D_{\mathrm{shell}}(i) = -\sum_{i=2}^{N} [D(i) - \widetilde{D}(i)]. \quad (10)$$

The result is shown in the upper part of Fig. 3. Here, the starting size for integration is 50, that is, we calculate $E_{\mathrm{shell}}(N) - E_{\mathrm{shell}}(50)$ and the base line for the shell energies is $E_{\mathrm{shell}}(50)$. This choice has no consequence for the amplitudes and the general shape of the E_{shell} function. Theoretical mean-field calculations, due to Frauendorf and Pashkevich,[11] are shown in the lower part of Fig. 3. Here a cluster temperature of 460 K is assumed in accordance with typical evaporation conditions.[14,15] The dashed line shows what the energy oscillations would be in the absence of deformations, whereas the full line (open circles) is the result of a variational calculation, where each cluster is allowed to relax to a minimum in energy under various axially symmetric deformations.[11] Deformations reduce the amplitudes in the shell energy oscillations by a factor of 2–3, as one sees. If one now compares with the experimental shell energies, which are plotted above using the same energy scale, it becomes clear that the observed oscillations are more correctly described when deformations are taken into account. We interpret this as an indication that these large clusters are deformed—except near shell closures. To our knowledge, this is the first quantitative evidence for deformation effects obtained so far for large clusters. The maximum cluster size, where deformations have been found previously, is $N = 48$. Here the deformation is reflected through a splitting of the plasmon peak into two components.[16,17]

The agreement between theory and experiment, Fig. 3, is not perfect. Whether this is due to experimental inaccuracies or to the neglect of nonaxial deformations, or both, is difficult to say at the moment.

A few comments may be in order. As already stated, the present analysis of the abundance spectra in terms of Eq. (9) is to our knowledge new. In a number of earlier studies of shells and supershells, shell closures and magic numbers have erroneously been identified with inflection points in the relative abundance spectra under the assumption that $\ln I_{\mathrm{rel}}(N) \sim D_{\mathrm{shell}}(N)$.[5,13] This assumption may well be valid for an ensemble undergoing evaporation in a heat bath, but, as we have stressed, it is not valid for evaporation *in vacuo*. Our treatment defines a shell closure rather as a maximum in the abundance. This does not affect the modulation in amplitude of the shell oscillations that constitute the supershell phenomenon. Nor does it change the specific signature of the supershell, i.e., the occurrence of a shift of half a shell period at the supershell node at $N = 900-1000$.[13,18] It does, however, lead to new magic numbers. It is therefore interesting to see how this affects a plot of shell index versus the cube root of magic numbers, $N_0^{-1/3}$. Table I shows the result of the analysis of our spectra for sizes up to the first supershell minimum using both definitions. In both cases the data can be fitted to a straight line, albeit with slightly different slopes as indicated on the bottom line of Table I. The slope in such a linear plot is interpreted in semiclassical theory as the signature of simple periodic orbits, characteristic of the mean

TABLE I. Magic numbers as deduced from the inflection points of the separation energy ($N_0^{D(N)}$) (new definition) compared to the inflection point of the abundances ($N_0^{I(N)}$) (old definition). The last line gives the slope of the best straight line fit when the cube root of the magic numbers is plotted as a function of the shell index.

Shell index	$N_0^{I(N)}$ (old)	$N_0^{D(N)}$ (new)
5	58	58
6	92	92
7	138	138
8	198±2	192±2
9	258±3	256±2
10	340±3	334±2
11	444±3	430±2
12	550±3	540±5
13	682±5	648±5
Slope	0.616±0.005	0.604±0.005

field in question. For spherical metal clusters, triangles and squares are predicted to contribute about equally to the observed shell modulations.[19] A triangular orbit, acting alone, would result in a slope of 0.630, whereas a square orbit would give a slope of 0.579, the mean value being 0.604. As one sees, the two experimental values in Table I are both quite close to the estimated mean value.

The present analysis is based on the assumption that evaporation of single atoms is the only open decay channel available for cooling the ensemble of initially hot clusters. Recently, experiments on fullerenes have shown that here heat radiation may be significant in shaping the abundance spectra.[20] The magnitude of this effect for our spectra was estimated by an analysis using the technique of Ref. 12, with the emissivity extrapolated from dielectric properties of bulk alkali metals. The result was that unless the emissivity varies very strongly with shell structure, radiative cooling does not play a role on time scales relevant for our experiment.

II. SHELL OSCILLATIONS IN THE ATOMIC SEPARATION ENERGIES AND IN THE IONIZATION POTENTIALS

Using the results from the first part of this work, we now want to examine the electronic shell oscillations in the ionization potentials and compare with the atomic separation energies derived from evaporation experiments in order to test the basic assumption used in analyzing these experiments, namely, that the observed abundance oscillations are of purely electronic origin.

In the photoionization experiments with alkali-metal clusters, the electronic shell structure is revealed directly as the characteristic oscillations of the ionization potentials relative to a smooth size dependence[3,21,22] in agreement with theoretical models of electrons moving in a spherical or deformed mean field.[23,24] The ionization potentials (IP's) are known for neutral sodium clusters Na_N with $N=1-106$ from measurements by two groups and presented in Fig. 4(a).[21,22] In one experiment, IP's were measured for the size range $N=1-22$ with clusters from an adiabatic expansion cluster source.[21] In the other experiment, measurements were done on cold sodium clusters from a laser vaporization cluster source for $N=9-106$ with some gaps in the low size range.[22] When the two sets of data overlap the lower value, obtained for the colder clusters, is selected. The experimental points in Fig. 4(a) present a smooth trend, well described by the relation

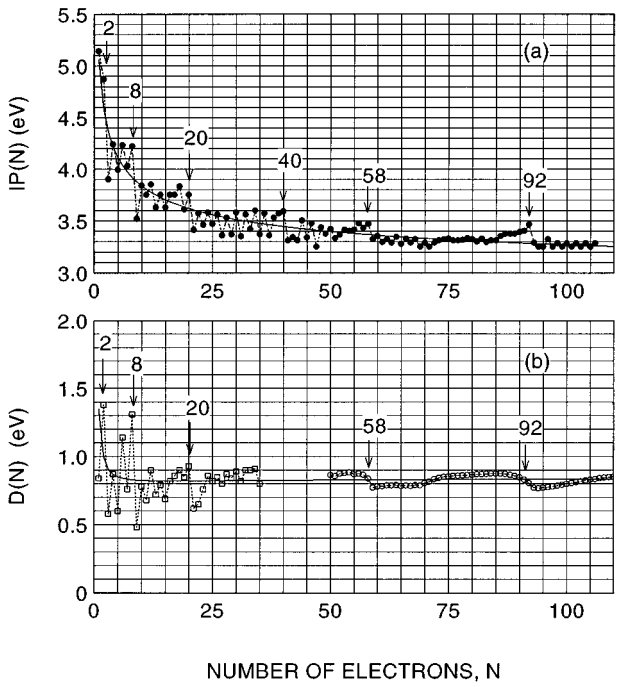

FIG. 4. (a) Experimental ionization potentials of neutral sodium clusters (Refs. 21 and 22) (●). The solid curve is the best fit to the experimental data using Eq. (11). (b) Experimental atomic separation energies of sodium clusters. The small size range (□) is for singly ionized clusters (Ref. 14), whereas the large one (○) refers to neutral clusters (this work). The solid line is the best fit to the small size data using Eq. (12).

$$\widetilde{IP}(N)=a+bN^{-1/3}, \tag{11}$$

where a and b are fit parameters.[25] The oscillating term $IP_{\text{shell}}(N)$ is extracted by fitting the smooth trend and substracting the fitted values from the experimental ones. The fit obtained is indicated on Fig. 4(a) and corresponds to $a=2.78$ eV and $b=2.28$ eV. To display the shell gaps in the oscillating term more clearly and in order to suppress the odd-even effect the function $IP_{\text{shell}}(N)+IP_{\text{shell}}(N-1)$ is actually used in the plot Fig. 5(a) instead of simply $IP_{\text{shell}}(N)$. The amplitudes corresponding to twice the shell gaps are indicated.

The same procedure is applied to the atomic separation energy $D(N)$. Two sets of data are also used here [see Fig. 4(b)] both obtained for hot, evaporating clusters (Ref. 14 and this work). One is deduced form photoevaporation experiments on size selected cluster ions $Na_{N'}{}^+$, for $N'=2-36$ (Ref. 14) (N' denotes the number of ions that differ from the number of electrons N by 1). Here, the shell term is extracted using the liquid drop model for the smooth part.[26,27] For a charged cluster $Na_{N'}{}^+$, the liquid drop expansion of the separation energy is of the form

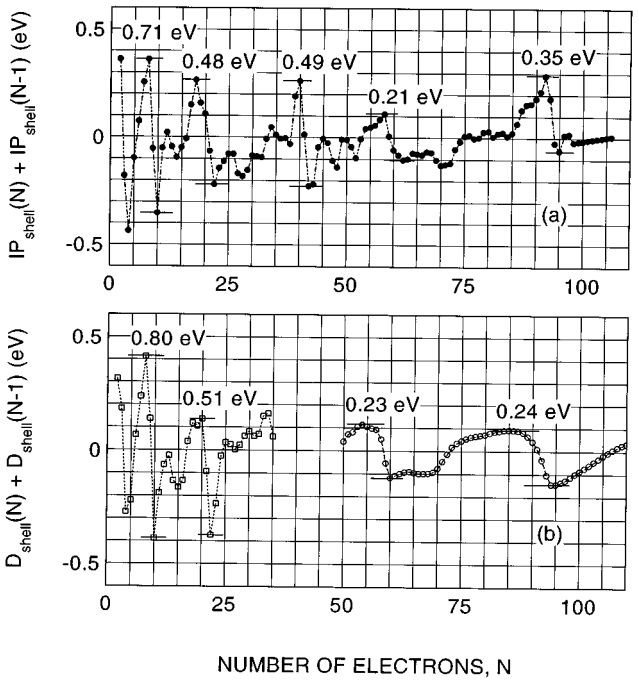

FIG. 5. (a) Shell oscillations in the ionization potential of sodium clusters based on the experimental data displayed in Fig. 4(a). The function $IP_{\mathrm{shell}}(N)+IP_{\mathrm{shell}}(N-1)$ is plotted to remove the odd-even effect. The amplitudes of the shell gaps are marked. (b) Same as in (a) for the atomic separation energy based on the experimental data displayed in Fig. 4(b).

$$\widetilde{D}(N')=a'-b'N'^{-1/3}+c'N'^{-4/3}, \tag{12}$$

where a', b', and c' are positive fit parameters. The best fit to the experimental points is shown in Fig. 4(b) and gives $a'=0.866$ eV, $b'=0.153$ eV, and $c'=0.636$ eV. The second set of data, for neutral sodium clusters Na_N for $N\gtrsim 50$, was obtained in the first part of this work. It yields a dimensionless separation energy $D_{\mathrm{rel}}(N)=D(N)/\widetilde{D}(N)$, which for the present purpose is normalized to the liquid drop value obtained by extrapolation from the small sizes. Again, in order to suppress the odd-even staggering and to exhibit the true shell effect more clearly the function $D_{\mathrm{shell}}(N)+D_{\mathrm{shell}}(N-1)$ is plotted as a function of the number of electrons N [see Fig. 5(b)], and the amplitudes of (twice) the shell gaps are indicated.

When comparing the functions $IP_{\mathrm{shell}}(N)+IP_{\mathrm{shell}}(N-1)$ and $D_{\mathrm{shell}}(N)+D_{\mathrm{shell}}(N-1)$ in Fig. 5, the general trends are seen to be very similar. In addition the magnitude of the shell steps at $N=8$, 20, 40, and 58 agree quantitatively within the experimental uncertainties. Fine details due to deformations are observed in both cases in the small size region and also the plateau after the shell closing at 58 is seen in both cases. On the other hand, for $N\gtrsim 50$, $D_{\mathrm{shell}}(N)+D_{\mathrm{shell}}(N-1)$ is much smoother than $IP_{\mathrm{shell}}(N)+IP_{\mathrm{shell}}(N-1)$ and for $N=92$, the step in the separation energies appears to be significantly smaller than in the case of the ionization potentials. This might be a consequence of the higher temperature of the clusters in the first case compared to the second, these effects being well known for large clusters from theoretical studies.[11] Finally there is some disagreement in the region just above $N\gtrsim 20$ that is not readily explained.

How can the agreement between the two curves be understood? The ionization potential is the energy needed to remove the least bound electron whereas the atomic separation energy is the energy needed to remove a neutral atom. On the average these two energies are very different, as can be seen from Fig. 4. Nevertheless, removing an atom can be also viewed energetically as first removing an electron, then removing an ion, and finally reforming the atom outside. The latter process yields a constant energy and cannot cause oscillations. If also the energy required to remove an ion is a smooth, nonoscillating function of size, it follows that only the first quantity, the electronic removal energy, should present shell oscillations. The comparison, Fig. 5, can be taken as evidence that the removal energy of an ion is indeed a nonoscillating function of size. Accepting this, the close agreement between the electronic separation energies in the two processes is all the more remarkable because the evaporation of an atom is a slow process involving the motion of the heavy positive ions across the cluster surface. The pertinent quantity that enters into $D(N)$ is therefore the adiabatic ionization potential (AIP). On the other hand, photoionization is a sudden process, and what should be probed here is the vertical ionization potential (VIP). The comparison in Fig. 5 can therefore be seen as comparing the influence of shell structure on the VIP and the AIP, respectively. As one sees, the two quantities are remarkably similar. Altogether the comparison serves to substantiate the interpretation of cluster evaporation spectra in terms of electronic shell structure.

CONCLUSION

In conclusion, we have shown that by using a simple formula and normalizing to the cohesive energy of bulk sodium, oscillations in the abundances of sodium clusters evaporating in vacuum can be converted to absolute separation energies and shell energies. The resulting shell energies are described quantitatively by theory, provided deformations are taken into account. It remains a challenge to understand the detailed nature of the deformations that nonmagic clusters assume.

ACKNOWLEDGMENTS

The authors wish to express special thanks to S. Frauendorf and V. V. Pashkevich for providing us with results of their theoretical calculations. We are also thankful to M. Brack and H. Busch for stimulating discussions. F. C. wishes to thank the Niels Bohr Institute for hospitality and Le Ministère des Affaires Etrangères of France for a grant under the Lavoisier program. Financial support of K. H. from the European Community under the Human Capital and Mobility programme is gratefully acknowledged. This work was supported by the Danish Natural Science Research Council and by the European Commission, Grants No. SC1-CT91-0654 and No. CHRX-CT94-0612.

*Present address: CEA Grenoble, DRFMC/SI2A, 17, rue des Martyrs, F-38054 Grenoble, France.
†Present address: Max Born Institut, Rudower Chaussee 6, Postfach 1107, 12474 Berlin, Germany.
[1] W. D. Knight, K. Clemenger, W. A. de Heer, W. A. Saunders, M. Y. Chou, and M. L. Cohen, Phys. Rev. Lett. **52**, 2141 (1984).
[2] K. Clemenger, Phys. Rev. B. **32**, 1359 (1985).
[3] W. A. de Heer, Rev. Mod. Phys. **65**, 611 (1993), and references therein.
[4] W. A. de Heer, W. D. Knight, M. Y. Chou, and M. L. Cohen, Solid State Phys. **40**, 93 (1987).
[5] S. Bjørnholm, J. Borggreen, O. Echt, K. Hansen, J. Pedersen, and H. D. Rasmussen, Z. Phys. D **19**, 47 (1991).
[6] S. Bjørnholm, J. Borggreen, H. Busch, and F. Chandezon, in *Large Clusters of Atoms and Molecules*, Vol. 313 of *NATO Advanced Studies Institute Series E: Applied Sciences*, edited by T. P. Martin (Kluwer Academic, Dordrecht, 1996), p. 111; F. Chandezon, P. Apesland, and T. Madsen (unpublished).
[7] C. E. Klots, J. Chem. Phys. **83**, 5954 (1985); Nature (London) **327**, 222 (1987).
[8] V. M. Strutinsky, Nucl. Phys. **A122**, 1 (1968).
[9] M. Brack, O. Genzken, and K. Hansen, Z. Phys. D **21**, 65 (1991).
[10] C. Bréchignac, P. Cahuzac, J. Leygnier, A. Sarfati, and V. M. Akulin, Phys. Rev. A **51**, 3902 (1995).
[11] S. Frauendorf and V. V. Pashkevich, in *Large Clusters of Atoms and Molecules* (Ref. 6).
[12] U. Näher, and K. Hansen, J. Chem. Phys. **101**, 5367 (1994); K. Hansen and U. Näher (unpublished); K. Hansen, in *Proceedings of the Seventh International Symposium on Small Particles and Inorganic Clusters, Kobe, 1994*, edited by Y. Nishina (World Scientific, Singapore, 1995), p. 597.
[13] S. Bjørnholm, J. Borggreen, O. Echt, K. Hansen, J. Pedersen, and H. D. Rasmussen, Phys. Rev. Lett. **65**, 1627 (1990); J. Pedersen, S. Bjørnholm, J. Borggreen, K. Hansen, T. P. Martin, and H. D. Rasmussen, Nature (London) **353**, 733 (1991).
[14] C. Bréchignac, P. Cahuzac, J. Leygnier, and J. Weiner, J. Chem. Phys. **90**, 1492 (1989); F. Carlier, Ph.D. thesis, Université de Paris Sud, Centre d'Orsay, 1989.
[15] K. Hansen and J. Falk, Z. Phys. D **34**, 251 (1995).
[16] K. Selby, V. Kresin, J. Masui, M. Vollmer, W. A. de Heer, A. Scheidemann, and W. D. Knight, Phys. Rev. B **43**, 4565 (1991).
[17] J. Borggreen, P. Chowdury, N. Kebaïli, L. Lundsberg-Nielsen, K. Lützenkirchen, M. B. Nielsen, J. Pedersen, and H. D. Rasmussen, Phys. Rev. B **48**, 17 507 (1993).
[18] T. P. Martin, S. Bjørnholm, J. Borggreen, C. Bréchignac, P. Cahuzac, K. Hansen, and J. Pedersen, Chem. Phys. Lett. **186**, 53 (1991).
[19] H. Nishioka, K. Hansen, and B. R. Mottelson, Phys. Rev. B **42**, 9377 (1990); O. Genzken, Mod. Phys. Lett. **7**, 197 (1993).
[20] E. Kolodney, A. Budrevich, and B. Tsipinyuk, Phys. Rev. Lett. **74**, 510 (1995); K. Hansen and E. E. B. Campbell, J. Chem. Phys. **104**, 5012 (1996).
[21] M. M. Kappes, M. Schär, U. Röthlisberger, C. Yeretzian, and E. Schumacher, Chem. Phys. Lett. **143**, 251 (1988).
[22] J. L. Persson, Ph.D. thesis, University of California, Los Angeles, 1988; R. Whetten (private communication).
[23] W. Ekardt, Phys. Rev. B **29**, 1558 (1984).
[24] M. Brack, Rev. Mod. Phys. **65**, 677 (1993).
[25] M. Seidl and J. P. Perdew, Phys. Rev. B **50**, 5744 (1994).
[26] M. Seidl and M. Brack, Ann. Phys. (N.Y.) **245**, 275 (1996).
[27] C. Bréchignac, in *Clusters of Atoms and Molecules: Theory, Experiment and Clusters of Atoms*, edited by H. Haberland (Springer-Verlag, Berlin, 1994), p. 255.
[28] C. Kittel, *Introduction to Solid State Physics* (Wiley, New York, 1986), pp. 99–124.